ELSEVIER

Journal of Crystal Growth 236 (2002) 647–654

JOURNAL OF CRYSTAL GROWTH

www.elsevier.com/locate/jcrysgro

Self-assembling quantum dot lattices through nucleation site engineering

B.D. Gerardot[a,*], G. Subramanian[b], S. Minvielle[a], H. Lee[a], J.A. Johnson[a], W.V. Schoenfeld[a], D. Pine[b], J.S. Speck[a], P.M. Petroff[a]

[a] *Materials Department, University of California, Santa Barbara, CA 93106, USA*
[b] *Chemical Engineering Department, University of California, Santa Barbara, CA 93106, USA*

Received 25 May 2000; accepted 24 December 2001
Communicated by A. Zangwill

Abstract

The long range ordering of epitaxial semiconductor quantum dots is investigated using several crystal growth techniques on prepatterned substrates. We have developed two nucleation site control techniques: one which uses localized surface chemical potential engineering and one which uses localized surface strain engineering. We present experimental results that demonstrate the ability to create ordered quantum dot lattices and discuss the different mechanisms involved in the long range ordering of quantum dots. © 2002 Elsevier Science B.V. All rights reserved.

Keywords: A1. Nanostructures; A1. Nucleation; A3. Molecular beam epitaxy; A3. Self-assembly; A3. Quantum dots; B2. Semiconducting III–V materials

1. Introduction

In the last few years, the "atom like" character of some of the electronic properties of semiconductor epitaxial self-assembled quantum dots (QDs) has been demonstrated through numerous spectroscopic experiments [1]. It is therefore compelling to try to order these QDs in a periodic lattice since the introduction of electronic coupling between QDs should lead to novel physical properties. An expected consequence of the three-dimensional (3D) electronic coupling is the formation of minibands, analogous to the 1D miniband case in semiconductor quantum wells. One also expects that carrier localization effects and optical properties will greatly depend on the QD lattice period and orientation. The metal or insulator behavior or carrier hopping transport regime will depend on the QD lattice band structure. One of the standard approaches to create QD lattices is to control the nucleation process for the QDs to the point where the lattice period, orientation and basis can be chosen at will.

Long range ordering of self-assembled quantum dots has remained until now a rather elusive and uncontrolled process. A simple reproducible method for producing self-assembled QD lattices

*Corresponding author. Tel.: +1-805-893-8300; fax: +1-805-893-8983.
E-mail address: gerardot@engineering.ucsb.edu (B.D. Gerardot).

0022-0248/02/$ - see front matter © 2002 Elsevier Science B.V. All rights reserved.
PII: S0022-0248(02)00849-7

has yet to emerge. Experiments on the Si/Ge system [2,3] and results on the GaAs/InAs system [4,5] suggest that the use of periodic strain fields is a viable approach to achieve QD self-ordering. One-dimensional QD ordering along the growth direction has been known for a long time and its modeling has clearly shown the role of the local strain on the QD nucleation process [6,7]. Hence, techniques that will create a periodic and localized strain on the surface should provide a way for creating a 2D lattice of nucleation centers. Another approach to ordering in densely packed QD arrays uses the propagation of the strain fields from closely spaced QDs as the growth proceeds from one layer of QDs to another. With this approach, the overlapped strain field of two closely spaced QDs will appear as a single nucleation center to the next layer of QDs that is grown in close proximity. This filtering action of the strain field from one layer to another leads to a short range ordering that has been demonstrated theoretically and experimentally in Si/Ge [8] and GaAs/InAs [9] systems.

A second technique for 2D ordering of self-assembled QDs is to use a directed migration of adatoms to a localized center. This can be achieved with localized surface chemical potential engineering [10,11]. By patterning the bulk surface, one can create a periodic array of localized centers having a lower chemical potential due to capillarity effects. This will create a driving force for adatom diffusion towards the center and cause island nucleation before the critical thickness for islanding in the bulk is realized. In this paper we will investigate the two techniques of nucleation site engineering to permit the growth of 2D lattices of QDs.

2. Experimental procedure

In all experiments we rely on the atomic force microscope (AFM) to establish the ordering of InAs islands on GaAs patterned surfaces. Prior to patterning a sample, an epi-GaAs layer was grown using MBE standard growth on a (1 0 0) GaAs substrate. After surface patterning using one of the techniques described below, a thorough solvent and quick O_2 plasma cleaning was performed followed by a 10 s diluted HCl (10% by volume) oxide etch. The patterned sample was then introduced into the MBE system. The oxide layer was carefully desorbed under an As_2 flux (9×10^{-6} Torr) at 635°C. In situ reflection high-energy electron diffraction (RHEED) was used to monitor the sample surface during the regrowth. A thin GaAs buffer layer was grown at 610°C prior to InAs deposition on all samples to preserve the surface patterned features. Multiple growth interruptions (10 s every 10 Å) were used during the buffer deposition to enhance surface recovery from desorption damage. After completing the buffer layer growth, the substrate temperature was lowered to 550°C and the InAs was deposited. Multiple growth interrupts (2 s every 0.1 monolayers (ML)) were used for the growth of the InAs. Due to the patterned surface profile of the samples, RHEED could not be reliably used during regrowth to monitor the onset of island nucleation. Therefore, a control InAs island sample was grown on a smooth surface prior to any sample regrowths to calibrate the 2D to 3D transition thickness as determined by RHEED.

2.1. Periodic strain engineering of the surface

The first method relies on the introduction of a lattice of strain centers at the surface. These strain centers are associated with a lattice of mesas defined on the GaAs surface [4,5]. The strain associated with each mesa is enhanced by the introduction of a coherently strained $In_{0.2}Ga_{0.8}As$ layer below the surface mesa. A 10 nm GaAs buffer layer and the InAs QD layer are deposited by MBE on top of the stressor film. The sample structure is schematically shown in Fig. 1.

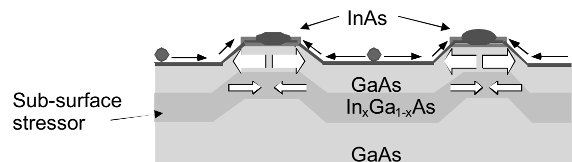

Fig. 1. Schematic of the periodically strained structure used in the growth of the QD lattice. Arrows indicate the $In_{0.2}Ga_{0.8}As$ subsurface is coherently strained to the GaAs surface.

Holography-based lithography [12] was used to define mesas with dimensions 150 nm × 150 nm and a mesa lattice period of ≈200–400 nm. The $In_{0.2}Ga_{0.8}As$ subsurface stressor film is coherently strained to the GaAs substrate as indicated schematically by the arrows in Fig. 1. During the stressor and buffer layer deposition, the mesas elongate along the [1 $\bar{1}$ 0], resulting in mesas with dimensions of 50 nm × 200 nm. The influence of the subsurface stressor film is illustrated in Fig. 2. Fig. 2A is an AFM image of the surface after depositing the InAs islands with no subsurface stressor. In the absence of the $In_{0.2}Ga_{0.8}As$ subsurface stressor, all the islands nucleate between the mesas. Fig. 2B shows an AFM image after InAs island formation on a sample with the subsurface stressor. The InAs islands nucleate on top of the mesas. The unit cell sides are aligned along ⟨1 0 0⟩ directions while the basis of the lattice is aligned along a ⟨1 1 0⟩ direction. The number of QDs for this size of mesas is either 1 or 2 per lattice point (Fig. 2B) and long range ordering is obtained over areas as large as a cm^2. By changing the mesa orientation we can change the lattice orientation and QDs lattices with unit cell vectors parallel to ⟨1 1 0⟩ or ⟨1 0 0⟩ or ⟨3 1 0⟩ have been obtained [4]. The number of islands on top of the mesa can be varied by adjusting the amount of InAs deposited.

2.2. Periodic surface patterning method

We have investigated two other lithographic techniques to create a periodically patterned surface for controlling QD nucleation. The first technique, shown schematically in Fig. 3, uses

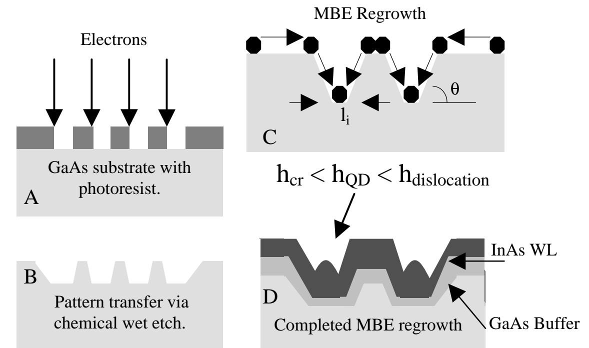

Fig. 3. Schematic of the periodic surface patterning process using electron beam lithography for producing ordered InAs islands. A photoresist is spun on a GaAs substrate and an electron beam patterns the resist (A). After developing, the pattern is transferred using a chemical wet etch (B). The patterned sample is then introduced into the MBE chamber for regrowth. After careful oxide desorption, an epi-GaAs buffer layer is deposited, then the InAs. The adatoms preferentially nucleate in the concave depressions (C), and the critical thickness for 3D growth is reached in the depression first (D). InAs deposition is stopped after island formation but before dislocations form.

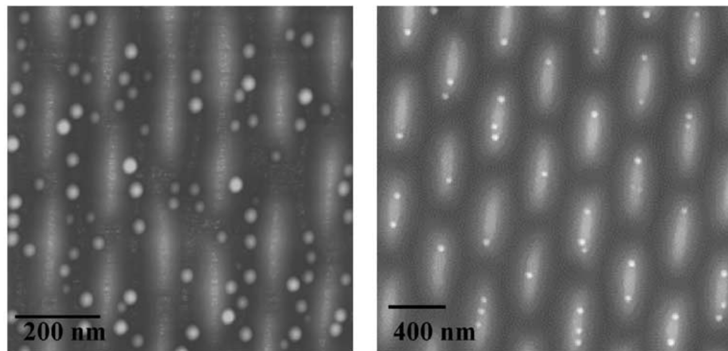

Fig. 2. AFM images (A (B)) showing the InAs islands nucleate between (on top of) the mesas in the absence (presence) of the $In_{0.2}Ga_{0.8}As$ subsurface stressor. The number of islands per lattice point can be controlled. In B there are 1–2 islands per mesa. The mesa lattice period is 200 (400) nm and the unit cell sides are aligned along ⟨1 0 0⟩ directions while the basis of the lattice is aligned along a ⟨1 1 0⟩ direction.

standard electron beam lithography and chemical wet etching to produce a periodic pattern of circular surface depressions with a diameter range of 100–400 nm and a pitch range of 0.5–4 μm. For fabrication of the patterns, the GaAs surface was spin-coated with 60 nm of polymethylmethacrylate (PMMA) positive electron beam resist (950k PMMA A 5.5 from MicroChem Corp, MA diluted to 2% in Anisole from Acros Organics, NJ). In a modified scanning electron microscope (Jeol JSM-840 modified by J.C. Nabity Lithography Systems, MT) dot patterns were exposed in an $80 \times 80\,\mu m^2$ field of view. After developing the resist, the patterns were transferred by etching ~ 50 nm into the epi-GaAs layer using a H_3PO_4:H_2O_2:$H_2O = 3{:}1{:}75$ wet chemical etch. The sample was then prepared for introduction into the MBE chamber. Deposition of the buffer layer introduced a faceting of the depression walls. We observed that the orientation and dimension of the depression strongly affects the arrangement of the InAs islands within the depression.

The two examples in Fig. 4 demonstrate that the In adatoms diffuse to the bottom of the concave depression. AFM data on the sample in Fig. 4A (Sample A) at the edge of the depression lattice show no island nucleation outside of the depressions with the exception of a few defects. AFM data at the edge of the depression lattice in Sample B (Fig. 4B), show no island nucleation within 15 μm of the patterned surface, suggesting an upper limit for the adatom diffusion length (L_D) of 15 μm. This estimate does not take into account the possible formation of immobile In clusters. It is also possible that this diffusion length is strongly affected by the presence of a strain gradient associated with the build up of the wetting layer prior to the formation of InAs islands. For Sample A, the amount of InAs deposited was 0.15 ML below the critical thickness for island formation on unpatterned substrates. In Sample B, the amount of InAs deposited was equal to the critical thickness for InAs island formation [13]. Other regrowths on patterned substrates with larger amounts of InAs resulted in higher densities of islands within the depressions and still no islands between the depressions.

The final technique for prepatterning the GaAs substrate used colloidal nanospheres as a lithography mask [14,15]. The main advantage of this technique is that a large monolayer array of hexagonally packed nanospheres can be used as a mask for patterning. The latex nanospheres are commercially available in a size range of 100–5000 nm. The disadvantages of the technique are: (a) the formation of domain walls in the nanosphere layer and (b) the difficulty in controlling the crystallographic orientation of the lattice. A schematic of the colloidal patterning process is shown in Fig. 5. A monodisperse latex sphere

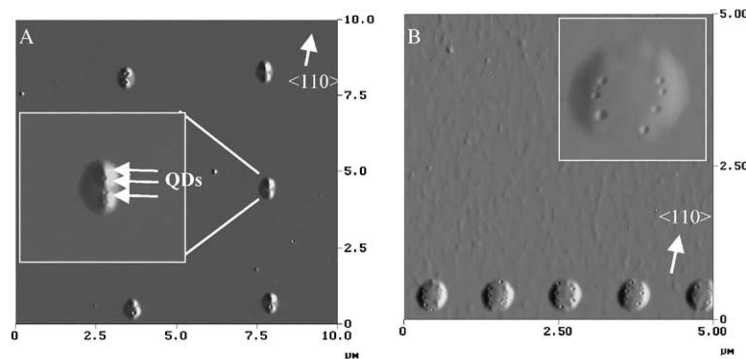

Fig. 4. (A) AFM micrograph of InAs islands deposited in a periodic lattice of depressions defined by chemical etching of a GaAs (1 0 0) surface. The depression lattice has a pitch of 4.0 μm and a GaAs buffer of 60 nm was deposited prior to an InAs regrowth (0.15 ml less than the critical thickness). No islands are observed anywhere on the sample except for in depressions and defects. (B) AFM micrograph from the edge of a different QD array with a 1.0 μm pitch. A GaAs buffer layer of 20 nm was used. The amount of InAs deposited was equal to the critical thickness. No islands were observed within 15 μm of the edge of a depression.

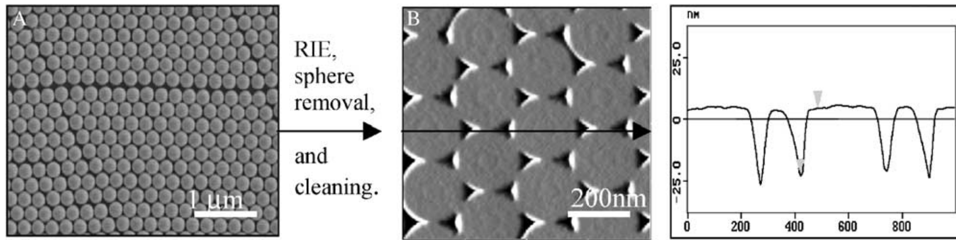

Fig. 5. Schematic of the latex colloidal patterning method. (A) SEM image of the colloidal monolayer on a GaAs substrate (sphere diameter = 240 nm). (B) AFM micrograph of the patterned substrate after RIE, sphere removal, and cleaning. Hexagonally ordered cylindrical GaAs posts are surrounded by triangular depressions. A cross-section of the line in (B) is shown in (C).

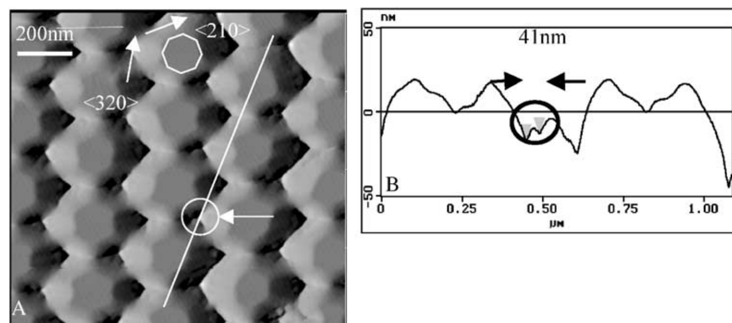

Fig. 6. (A) AFM micrograph after MBE regrowth. A 15 nm GaAs buffer layer was deposited prior to the InAs. The InAs islands preferentially nucleate in the honeycomb lattice of triangular depressions. (B) AFM cross-section along the line drawn in (A), with the noted island diameter.

suspension ($\sim$4% solids volume fraction) with a small amount of surfactant (TritonX-100) was coated on a MBE grown epitaxial GaAs film. The surfactant was used to increase wetting on the hydrophobic GaAs. Upon drying, the latex spheres are driven by capillary forces to form hexagonally ordered monolayers on the substrate. The orientation of the hexagonally closest packed 2D sphere lattice with respect to the GaAs surface crystallographic axis was not controlled in these experiments. The ordered layer of spheres was then directly used as an etch mask (Fig. 5A–B). Etching was done with a mixture of boron trichloride and chlorine in a Plasma Therm Series Reactive Ion Etching system at a pressure of 3 mTorr and a gas flow rate of 8 sccm (BCl_3 = 7 sccm, Cl_2 = 1 sccm). A RF power of 100 W was employed to achieve an etch depth of $\sim$35 nm with 240 nm spheres as the mask. We have found that the etch depth strongly depends on the diameter of the latex spheres. Smaller spheres tend to produce smaller etch depths for the same conditions due to reactant transport limitations. On subsequent removal of the spheres and cleaning of the substrates, ordered posts of GaAs surrounded by triangular depressions $\sim$35 nm in depth were obtained. The depressions themselves were arranged in a honeycomb lattice. Latex spheres with diameters ranging from 140 to 1000 nm were used to produce patterns with different length scales. The clean patterned substrates were then carefully desorbed and regrown by MBE. Once again a GaAs buffer layer is regrown after oxide desorption. Fig. 6(A) shows an AFM micrograph in which the InAs islands preferentially nucleate in the honeycomb packed depressions. This result corresponds to the regrowth of a 15 nm GaAs buffer and the InAs deposition. Fig. 6(B) shows the cross-section along the line in Fig. 6(A). The InAs island has a diameter of 41 nm. Faceting of the spherical posts is observed along the $\langle 3\,2\,0 \rangle$ and $\langle 2\,1\,0 \rangle$

directions. If a thicker buffer layer ($\geqslant$30 nm) is regrown, the amount of faceting is reduced and the islands form more randomly (both inside and outside of the depressions).

3. Discussion

In the techniques presented in this paper, positioning of self-assembled nanostructures is a result of the directed atomic diffusion and nucleation on the surface. After surface diffusion, atoms come to rest at equilibrium points on the surface and the island nucleation takes place to minimize the local energy of the epitaxial film [16–18]. One way to control adatom migration is to use a gradient in the chemical potential. Introducing a patterning on the surface can create a chemical potential gradient. Herring showed that for a convex surface neighboring a concave surface, matter diffuses from the convex surface towards the concave part to reduce the crystal's surface energy [19]. For a binary alloy (such as InAs), the chemical potential on a facet i surrounded by two sidewalls s misoriented by the same angle θ with respect to the horizontal can be written as

$$\mu_i = \mu_0 - \frac{\gamma \Omega_0}{l_i}, \quad (1)$$

where μ_0 is the chemical potential for a uniform surface, $\gamma = 2\,(\gamma_s \csc\theta - \gamma_i \cot\theta)$, γ_s and γ_i are the surface free energy of the sidewalls and facet i, respectively, Ω_0 is the atomic volume, l_i is the width of the facet, and the minus sign refers to a concave surface profile (Fig. 3). Under the associated driving force the material will preferentially accumulate at the bottom of the depressions. Once the critical layer thickness is achieved in the concave regions, an island or islands will nucleate to relieve the local build up of strain.

During deposition of the GaAs buffer layer onto the patterned surface, the shape and depth of the depression change, as a result of faceting. Fig. 4(A) shows an AFM image after a 60 nm GaAs buffer, and Fig. 4(B) shows the result after only 20 nm of buffer. The 20 nm GaAs buffer layer (Fig 4B) shows that sidewalls form and the depression elongates along the $\langle 1\,0\,0 \rangle$. After a 60 nm GaAs buffer layer deposition, the sidewalls have contacted each other, resulting in a V-groove parallel to $\langle 1\,0\,0 \rangle$. Ozdemir et al. [20] considered epitaxial growth onto non-planar substrates and found that when each facet in a non-planar profile has nearly the same growth rate, an originally flat-bottomed depression will evolve into a V-groove at intermediate times before planarization. Our AFM results are in agreement with this model.

Due to the surface chemical potential gradient, In adatoms within a diffusion length of a depression have a large chance of diffusing to it. Depressions with a larger surrounding collection area (adatom reservoir) will collect more atoms and should have a higher density of islands. AFM statistics on the electron-beam-patterned samples were collected to explore the effect of the adatom reservoir size on the island density. Two patterned samples, one with a 1.0 μm pitch and the other with a 2.0 μm pitch, were regrown simultaneously. The patterned area in each case was $80 \times 80\,\mu m^2$ and the diameters of the depressions were identical. The amount of InAs deposited was equal to the critical thickness on a planar surface. The mean number of islands per depression (IPD) at the center of the 1.0 μm pitch sample is 7.71, with a standard deviation $\sigma = 2.24$. The edge regions of the same sample have a mean IPD of 9.25 ($\sigma =$ 1.96). The center region of the sample with 2.0 μm pitch has a mean IPD of 8.60 ($\sigma = 2.29$). The data, presented in Fig. 7A and B, show there exists a higher density of islands per depression at the periphery of the depression lattice compared to the center. The identical effect is observed in depression lattices with a larger period (Fig. 7C). This effect is associated with the larger reservoir of In atoms available to the edge depressions and depression lattices with a greater pitch and the large diffusion length of the In adatoms.

This work demonstrates that long range ordering of self-assembled QDs is achievable using surface strain engineering. Three types of substrate prepatterning (electron beam lithography, colloid spheres, and holography) were used to create a lattice of nucleation sites for QDs during MBE regrowth. One of the nucleation site control techniques relies on the relaxation of strain at the top of mesas due to a buried stressor to cause

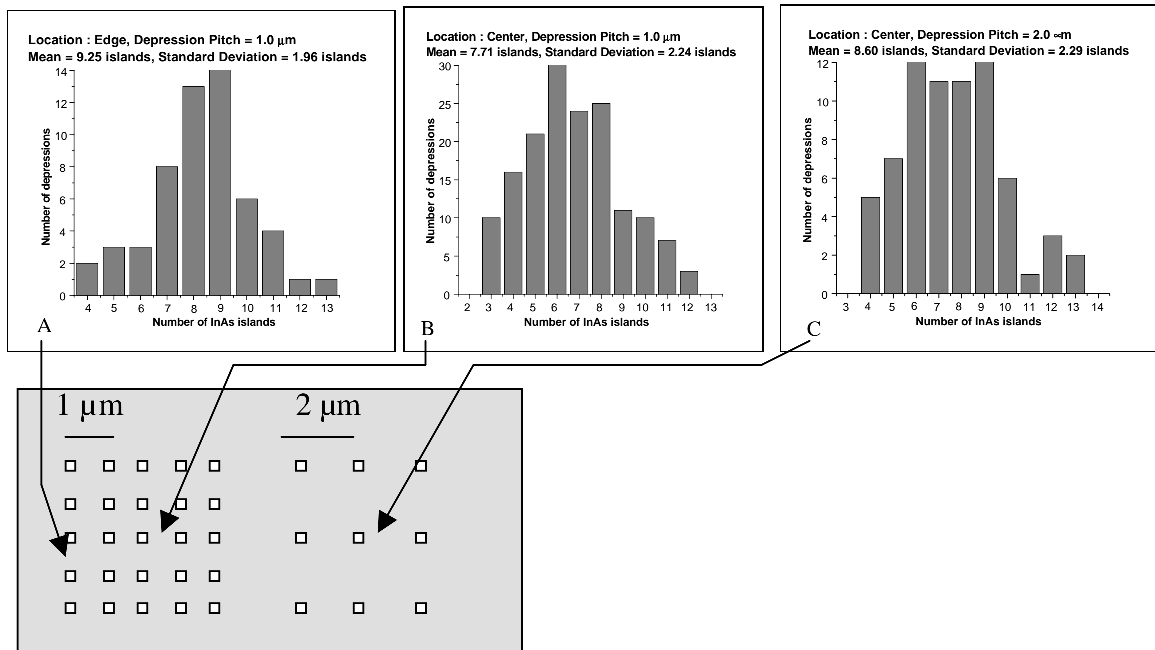

Fig. 7. Histograms of the number of InAs islands per depression measured by AFM at the (A) edge (IPD = 9.25) and (B) center (IPD = 7.71) of a 1.0 μm pitch lattice. (C) Histogram for the center of a 2.0 μm pitch lattice (IPD = 8.60). The results show that there is a higher density of islands per depression at the edges of a patterned area compared to the center area and also a higher density in depressions with a larger pitch.

preferential island nucleation on the mesas. The other two techniques rely on the introduction of a gradient in surface chemical potential to drive adatom diffusion to the bottoms of concave depressions. The results demonstrate the ability to fabricate QDs lattices and to control their lattice parameter, orientation, and basis. The limitation of either the surface strain or chemical potential engineering is the resolution of the lithography technique used for patterning. The greater the lithographic resolution (down to the size of an individual island), the more precise the QD location can be controlled. Future work will be aimed at using these techniques to achieve QD lattices with smaller periods (30–50 nm).

Acknowledgements

This research was supported by the following grants: ARO (Grant No. DAAD19-99-1-0372), AFOSR (Grant No. F49620-98-1-0367), ARO/MURI (Grant No. DAAG55-98-1-0366), and MRSEC (Grant No. DMR-9632716).

References

[1] H. Drexler, D. Leonard, W. Hansen, J.P. Kotthaus, P.M. Petroff, Phys. Rev. Lett. 73 (1994) 2252;
R.J. Luyken, A. Lorke, A.O. Govorov, J.P. Kotthaus, G. Medeiros-Ribeiro, P.M. Petroff, Appl. Phys. Lett. 74 (1999) 2486.

[2] G. Springholz, V. Holy, M. Pinczolits, G. Bauer, Science 282 (1998) 734.

[3] O.G. Schmidt, N.Y. Jin-Phillipp, C. Lange, U. Denker, K. Eberl, R. Schveiner, H. Gräbeldinger, H. Schweizer, Appl. Phys. Lett. 77 (2000) 4139.

[4] H. Lee, J.A. Johnson, J.S. Speck, P.M. Petroff, J. Vac. Sci. Technol. B 18 (2000) 2193;
H. Lee, J.A. Johnson, J.S. Speck, P.M. Petroff, Appl. Phys. Lett. 78 (2001) 105;
P.M. Petroff, A. Lorke, A. Imamoglu, Phys. Today 54 (2001) 46.

[5] A. Konkar, A. Madhukar, P. Chen, Appl. Phys. Lett. 72 (1998) 220.
[6] Q. Xie, A. Madhukar, P. Chen, N.P. Kobayashi, Phys. Rev. Lett. 75 (1995) 2542.
[7] G.S. Solomon, J.A. Terza, A.F. Marshall, J.S. Harris Jr., Phys. Rev. Lett. 76 (1996) 952.
[8] J. Tersoff, C. Teichert, M.G. Lagally, Phys. Rev. Lett. 76 (1996) 1675.
[9] G.S. Solomon, S. Komarov, J.S. Harris Jr., J. Crystal Growth 201/202 (1999) 1190.
[10] S. Jeppesen, M.S. Miller, D. Hessman, B. Kowalski, I. Maximov, L. Samuelson, Appl. Phys. Lett. 68 (1996) 2228.
[11] J. Heath, R. Williams, J. Shiang, S. Wind, J. Chu, C. D'Emic, C. Stanis, J. Bucchignano, J. Phys. Chem. 100 (1996) 3144.
[12] G. Gigli, R. Rinaldi, C. Turco, P. Visconti, R. Cingolani, F. Cacialli, Appl. Phys. Lett. 73 (1998) 3926.
[13] D. Leonard, K. Pond, P.M. Petroff, Phys. Rev. B 50 (1994) 11687.
[14] H.W. Deckman, J.H. Dunsmuir, Appl. Phys. Lett. 41 (1982) 377.
[15] F. Burmeister, C. Schafle, T. Matthes, M. Bohmisch, J. Boneberg, P. Leiderer, Langmuir 13 (1997) 2983.
[16] D.S. Mui, D. Leonard, L.A. Coldren, P.M. Petroff, Appl. Phys. Lett. 66 (1995) 1620.
[17] G. Biasiol, K. Leifer, E. Kapon, Phys. Rev. B. 61 (2000) 7223.
[18] A. Madhukar, K.C. Rajkumar, P. Chen, Appl. Phys. Lett. 62 (1993) 1547.
[19] C. Herring, in: W.E. Kingston (Ed.), The Physics of Powder Metallurgy, McGraw-Hill, New York, 1951, pp. 143–156.
[20] M. Ozdemir, A. Zangwill, J. Vac. Sci. Technol. A 10 (1992) 684.